

Experimental and Theoretical Investigation on Masonry after High Temperature Exposure

S. Russo · F. Sciarretta

Received: 2 July 2010 / Accepted: 27 March 2011 / Published online: 21 April 2011
© Society for Experimental Mechanics 2011

Abstract The results of experimental investigation on the mechanical properties of clay brick masonry after high temperature exposition are here presented. The adopted physical model of masonry means to represent both new and old load bearing walls, so to get useful and applicable results. Uniaxial and diagonal compressive tests were carried on masonry samples exposed to 300 and 600°C. Samples of the component materials were tested in compression as well, and the elastic moduli of bricks and mortar were also measured. The results allow to evaluate the levels of residual strength and stiffness of all tested materials after exposure to high temperatures. Finally, property-temperature laws of mechanical decay for masonry, brick and mortar after high temperature exposition are here proposed and discussed.

Keywords Brick masonry · High temperatures exposition · Residual properties

Notation

Subscript θ	denotes residual values of properties at temperature θ
E	Initial elastic modulus of masonry (N/mm ²)
E_{sec}	Secant elastic modulus of masonry at the maximum stress (N/mm ²)
E_b	Initial elastic modulus of brick (N/mm ²)
E_m	Initial elastic modulus of mortar (N/mm ²)
f_c	Compressive strength of masonry (N/mm ²)
f_v	Shear strength of masonry (N/mm ²)

f_{bc}	Compressive strength of brick (N/mm ²)
f_{bt}	Tensile strength of brick (N/mm ²)
f_{mc}	Compressive strength of mortar (N/mm ²)
f_{mf}	Flexural strength of mortar (N/mm ²)
G	Shear modulus of masonry (N/mm ²)
γ	Shear strain
γ_1	Peak shear strain
ε	Normal strain
ε_{c1}	Peak compressive strain of masonry
ε_{c2}	Ultimate compressive strain of masonry (at 50% of the peak stress, in the post peak branch)
θ	temperature (°C)
ν	Poisson's ratio of masonry
σ	Normal stress (N/mm ²)
τ	Shear stress (N/mm ²)

Introduction

Masonry buildings are often very vulnerable to fire, and—in the frequent case of historic masonry buildings—the need for fire protection may be in conflict with preservation issues; moreover, in the case of fire events in historic-cultural heritage buildings—which are unique and of public interest—equal importance should be effectively stated for the safeguard of the building and the safety of people [1–3].

On the other hand, the excellent behaviour of masonry walls and structures in fire and high temperature conditions is often highlighted by real events as well as fire testing [4, 5]. However, in some cases, code prescriptions (for both new and existing buildings) require also the structural safety after a fire event to be evaluated whenever high levels of fire safety are required by the client. Historic-cultural heritage

S. Russo · F. Sciarretta (✉)
Research Unit CdSM—“Assessment of monumental buildings”,
IUAV University of Venice,
Dorsoduro 2206,
30123 Venice, Italy
e-mail: scifra@iuav.it

buildings should need such evaluation, in order to ensure the preservation of a public property after fire events; as well, new buildings made of traditional masonry materials need careful design, expensive construction and expert workmanship, resulting in precious and representative works.

The post-fire reliability of masonry structures is thus a challenging field of research; the main difficulties lie in the expensiveness of testing, the complexity of physical and numerical modelling of a composite material, and the extensibility of experimental and numerical results. A few information is available as a basis to evaluate the effects of a fire—that is meaning an accidental exposure to high temperatures—on the residual safety of a masonry building. Research in this field would be useful to structural design in a general sense, including new constructions and repair of existing buildings, and would deal with theoretical and experimental study of masonry, testing-based design and evaluation of reliability with respect to accidental situations. Being a composite material, masonry features a great variety of block-joint combinations; this can limit the extent of experimental results, depending on the chosen materials, wall thickness and texture; cracking and damage phenomena must be investigated with accurate displacement control, in order to clarify the post peak behaviour in compression and in shear. The theoretical or theoretical-experimental research on constitutive laws for masonry in compression is nowadays a lively branch of study.

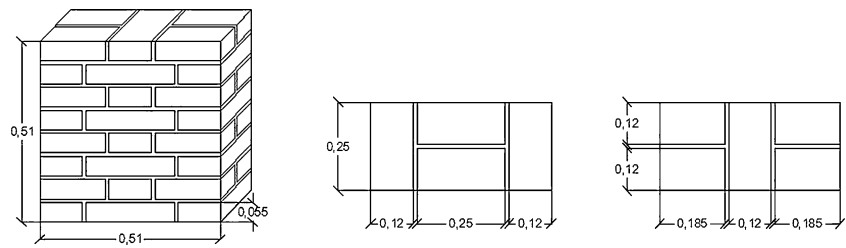
This paper focuses on materials' mechanical behaviour after exposure to high temperatures, which—for the above mentioned reasons—is much less investigated than fire endurance and performance of structural members under fire conditions. Outcomes of a research in progress at the IUAV University of Venice on the mechanical behaviour of masonry damaged by exposition to high temperatures [6] are here reported. Aspects in the field of civil engineering—mechanical characterisation and theoretical analysis of results—are here dealt with, in the case of masonry. The whole research consists of experimental phases regarding specific physical models, i.e. 1) load-bearing fire-separating wall 25 cm thick, 2) load-bearing fire-separating wall 38 cm thick, 3) load-bearing non-separating wall 25 cm thick, 4) load-bearing non-separating wall 38 cm thick, with the same component materials (brick and mortar) and exposure conditions (maximum temperature, duration and heating rate) in all. The experimental information is collected in order to elaborate and refine a theoretical-experimental model describing the mechanical behaviour of brick-mortar masonry after exposure; the first experimental phase and the first subsequent theoretical efforts are here referred to. The results mean to be useful in understanding the residual mechanical performance of masonry after high temperature exposure, especially for the purpose of post-fire assessment of masonry structures requiring high levels of fire safety.

Analogous work was done in the past and recently for concretes, high performance concretes and mortars by many authors [7–15], who tried to establish relationships between the parameters of high temperature exposure (maximum temperature, heating rate, duration at maximum temperature and cooling regime) and the consequent decay of mechanical parameters. Recommendations about test parameters and procedures in post-exposure conditions are also available for concrete [16], but not for masonry materials.

Available data on the temperature history of real fire events in ordinary buildings are scarce; some hints are given in [17]. Currently, theoretical research is still mainly focused on masonry walls' performance during fire exposure [18, 19], while very few experimental data are available on the residual mechanical properties of masonry and its components after fire exposure. It can be said that cement masonry materials (e.g. mortars, concrete or calcium silicate blocks) generally undergo a decrease in mechanical performances after high temperature exposure [7, 8]. Clay bricks of a historical masonry building subjected to a severe fire have shown an increase in stiffness and strength and a decrease in strain capacity [5, 20]. Data from research on concrete materials after fire exposure underline the major role of the maximum temperature in the residual mechanical properties and point out the additional importance of other factors (e.g. hydration rate and cooling regime) [7, 9, 10]. Besides, these researches have assessed the relevance of the component materials in the residual mechanical performance, e.g. concretes with different types of aggregate often show different performances under the same conditions [7].

Based on the experimental results here presented, functions of parameters' mechanical decay have been set up for masonry materials after high temperature exposition. The whole research refers to one physical model of masonry and aims to evaluate the influence of maximum temperature on the residual mechanical performance in compression and in shear. The choice of the mechanical parameters to be investigated was driven by two reasons. First, a quick and simple mechanical characterisation of masonry and its components was needed, resulting in the knowledge of the basic parameters of masonry design (compressive strength and pure shear strength) for each case of exposure, with the usual standard mechanical tests; then, additional experimental information (elastic modulus and strain properties both in compression and in shear), was yielded—by means of displacement control—to provide a basis for linear and nonlinear numerical modelling of masonry, which was developed in another part of the research [1]. Concerning the parameters of exposure, it was decided to focus only on maximum temperature, and to fix the heating rate and duration at maximum temperature in

Fig. 1 25 cm thick masonry specimens



order to simulate an accidental exposure with fast heating and short-term exposure at temperatures in the range 20–750°C at least, according to the RILEM recommendations for concrete [16]; two values of maximum temperature were thus taken into account, i.e. 300 and 600°C; such values belong to a low-medium range of high temperatures, since real fires in civil buildings can often reach higher temperatures (1000–1200°C). The two exposure conditions do not mean to represent all possible severe situations, but to provide a basis for the first investigation at a low-medium level of exposure.

Testing Programme

The physical model refers to masonry 25 cm thick, made of hand-made type clay bricks (sized 250×120×55 mm) and cement mortar, with joints 1 cm thick, assembled in the so-called ‘gothic bond’ pattern (in each row, alternate ‘heads’ and the ‘sides’ of the bricks are visible); square specimens of 51×51×25 cm were built (Fig. 1). Attention was paid to the selection of materials, masonry thickness and pattern, in order to represent a type of load-bearing masonry wall which could be common both to traditional and new buildings. These bricks are suitable for load-bearing walls, as they are similar to ancient ones in composition, dimensions and crafting process. A cement mortar classified as M10 following the standard UNI EN 998–2 was chosen because of its wide diffusion in existing load-bearing masonry structures in Italy; it is made of cement, hydraulic lime and sand in the proportions of 1 : 0.5 : 4.

Usual and simple tests following UNI standard procedures for masonry, bricks and mortar were planned, to get a quick mechanical characterization. Compressive and diagonal compressive tests were thus performed on masonry samples, flexural and compressive tests on mortar samples and compressive tests on brick samples. The initial elastic moduli in compression were also measured on samples of brick and mortar. Each type of test was performed on exposed and unexposed materials.

Two time-temperature curves were set up, each one expressing an exposure condition represented by the maximum temperature (300 and 600°C), with the same heating rate (about 19°C/min) and duration at maximum

temperature (1 h). Following also other authors’ procedures [10, 12] the heating rate was decided to be as high as possible, in order to simulate a fast rise of temperature; as well, in order to reflect an accident condition such as fire, a very short exposure was established. The time-temperature curves representing the two conditions are shown in Fig. 2.

Ten samples were exposed to high temperatures following each of the two curves. In order to simulate the case of a wall exposed to fire on one side, i.e. load-bearing separating wall, as it is contemplated in Eurocode 6 1:2 [21], the samples were covered in fire-resistant rock wool claddings which left just one of the largest faces free to exposure, as it is shown in Fig. 3. At the same time, samples of bricks and mortar were also exposed to the two thermal cycles; the largest faces of the bricks were insulated too, so to simulate the heating of an element within a masonry assembly. Since the material samples had been stored indoor within a dry environment, they were cured in water—masonry samples for 12 h, bricks and mortar prisms for 2 h—before the thermal cycle, so to attain a uniform level of water content.

The high-temperature exposure cycle was performed by means of a brick furnace, normally used for baking hand-made clay products. This oven ensured a quick heating process, a duration at a well approximately constant maximum temperature, and a uniform internal temperature; it allowed for all ten samples in each thermal cycle to be exposed. The temperature of the specimens during the exposure was recorded by means of nine thermocouples applied to three masonry specimens—one on a brick, one on the central bed joint and the last on the unexposed side, each inserted in a 7 mm deep hole (Fig. 4); another thermocouple was used to record the air temperature inside

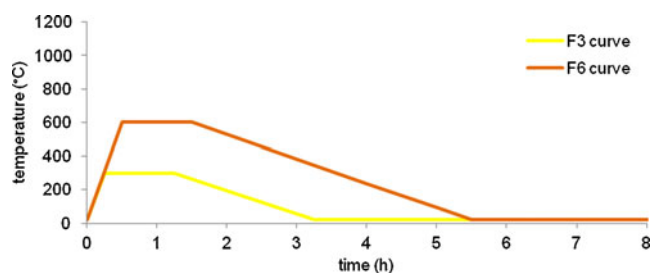


Fig. 2 Time-temperature curves of the two exposure conditions

Fig. 3 Masonry specimens being put inside the oven



the oven. It can be noticed that the real time-temperature curve fits with good approximation the prescribed one, until cooling begins; the temperature on the insulated side remains about 400°C lower than the air temperature, so that an appropriate simulation of the load-bearing separating wall is attained (Fig. 5).

Finally, a slow air-cooling process simulated a fire self-extinguishment, by turning off the furnace just after the duration at maximum temperature was completed; the door of the oven was opened 12 h later.

Just after the 300°C cycle, the exposed faces of the masonry specimens showed very little damage, i.e. some detachments at brick-mortar interfaces; after the 600°C exposure, interface cracking and micro-cracking in all materials (including bricks and mortar specimens) were clearly visible (Fig. 6). After removal of rock wool claddings, in both cases of exposition, the insulated faces of the masonry samples looked undamaged.



Fig. 4 Masonry specimen with applied thermocouples

Experimental Results

The mechanical testing programme was carried out at the Laboratory of Strength of Materials (LabSCo) at the IUAV University of Venice. In the following subsections, unexposed masonry, bricks and mortar are denoted with NF, while materials exposed to 300°C and 600°C are referred to as F3 and F6 respectively.

Brick and Mortar Specimens

Brick specimens and 4×4×16 cm prismatic mortar samples were employed for testing exposed and unexposed materials. All these tests were performed with a 200 kN maximum load testing machine (Galdabini SUN/20).

Compressive tests on bricks were carried out following UNI EN 772–1 standard procedure, to obtain the mean

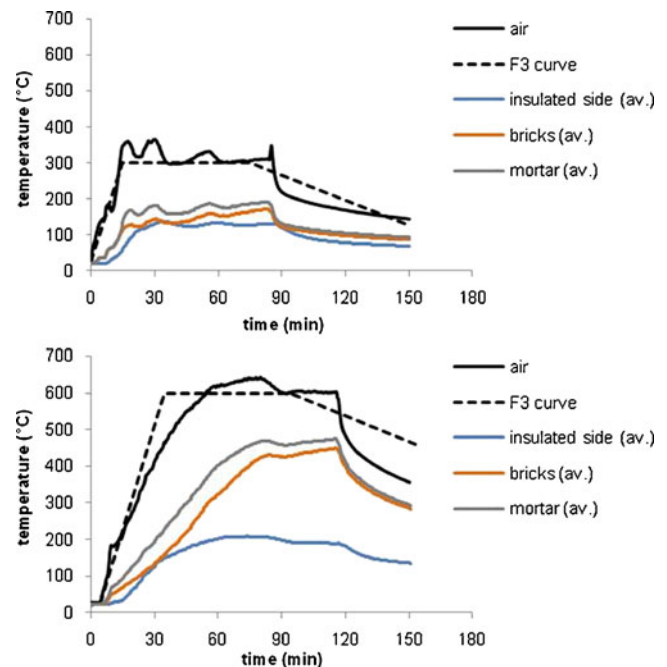
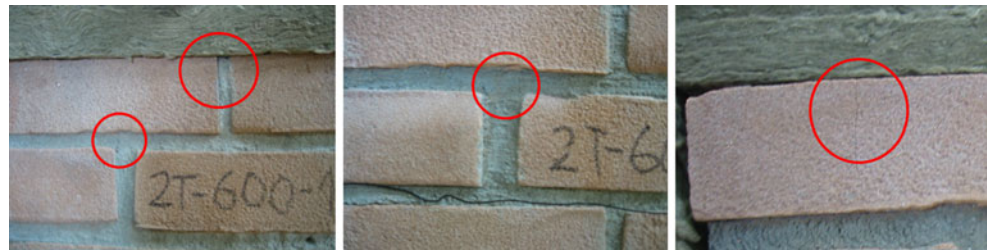


Fig. 5 Time-temperature graphs of the cycles compared to the prescribed curves

Fig. 6 Cracking and interface detachment on 600°C (F6) exposed masonry specimens



compressive strength $f_{bc,\theta}$; cubic samples were cut from exposed and unexposed bricks and dried before testing. Table 1 reports the compressive strength data. The elastic modulus of bricks $E_{b,\theta}$ was evaluated on $2 \times 2 \times 5$ cm specimens, according to UNI 9724 prescriptions; the vertical strain of each specimen was recorded by two electric strain gages. Table 2 reports the results of those tests, and Fig. 7 shows the corresponding stress-strain diagrams up to specimens' failure; the strain is the average of the two series of values recorded. The tests show a decrease in strength (−9% for F3 and −38% for F6 bricks) and a slight increase in stiffness (+15% for F3 and +1% for F6 bricks). The progressive decay in compressive strength of bricks is similar to the trend observed in concretes [7, 12, 13], and especially in siliceous aggregate concrete; this can

Table 1 Experimental data of compressive tests on brick samples

Compressive tests—BRICKS		
Sample	Dimensions (mm)	$f_{bc,\theta}$ (N/mm ²)
B-NF-1	48×48×49	19.69
B-NF-2	45×45×45	18.58
B-NF-3	47×47×47	19.25
average NF		19.17
standard deviation NF		0.456
relative standard deviation NF		0.024
B-F3-1	53×52.5×52.5	16.73
B-F3-2	54×53×53	18.32
B-F3-3	54×54×53	18.44
B-F3-4	54×55×53	16.84
B-F3-5	54×55×52.5	16.64
average F3		17.39
standard deviation F3		0.80
relative standard deviation F3		0.046
B-F6-1	54×54×54.5	13.76
B-F6-2	54×55×55	12.48
B-F6-3	55×55×54.5	12.02
B-F6-4	56×54×56	11.87
B-F6-5	53×54×55	9.67
average F6		11.96
standard deviation F6		1.324
relative standard deviation F6		0.1107

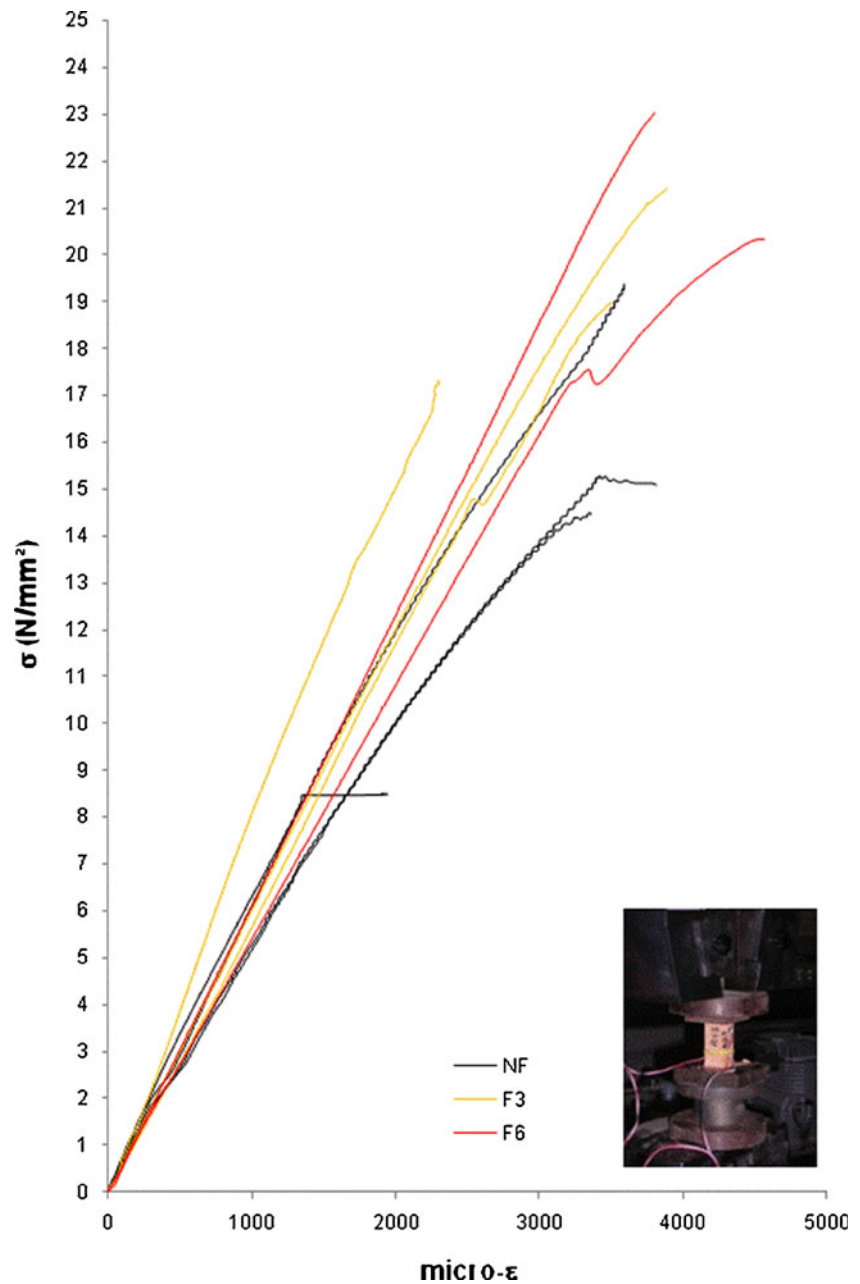
be due to the bricks' high content in silicates; concerning elastic modulus, an increase after exposure to a real fire—whose temperature history was not precisely known—was already observed in the bricks of a historic structure, although accompanied by an increase also in compressive strength [5].

The tests on mortar were carried out following UNI-EN 1015–11 standard; first, the prismatic samples were subjected to bending test, then the two halves of each one were tested in compression. The denominations and data about the mortar samples are recorded in Table 3, where $f_{mf,\theta}$ and $f_{mc,\theta}$ are respectively the flexural and the compressive strength of mortar. Elastic moduli $E_{m,\theta}$ of exposed and unexposed mortar were tested on the same specimens before the destructive tests; the vertical strain of each specimen was recorded by two 60 mm electric strain gages and the load was applied until half of the expected compressive strength was reached, so not to damage

Table 2 Experimental data of elastic modulus testing on brick samples

Elastic modulus—BRICKS	
Specimen	$E_{b,\theta}$ (N/mm ²)
B-NF-1E	6606
B-NF-2E	5082
B-NF-3E	5162
B-NF-4E	5991
average NF	5710
standard deviation NF	646.004
relative standard deviation NF	0.113
B-F3-1E	7934
B-F3-2E	5754
B-F3-3E	5986
average F3	6558
standard deviation F3	977.578
relative standard deviation F3	0.149
B-F6-1E	5986
B-F6-2E	5405
average F6	5765
standard deviation F6	4079.465
relative standard deviation F6	0.708

Fig. 7 Stress-strain diagram of elastic modulus tests on bricks



specimens before flexural and compressive tests. The stress-strain diagram of these tests is depicted in Fig. 8 and the corresponding data are listed in Table 4. The tests point out a clear increase in compressive strength (+29%) of F3 samples and an equal decrease of F6 samples; while the flexural strength decreases in F3 (−23%) and especially in F6 samples (−61%) which is greater in bending than in compression; the elastic modulus undergoes a considerable decrease as well (−10% in F3 and −51% in F6 samples).

The increase in compressive strength at 300°C here observed (and subsequent decrease at 600°C) agrees with what is reported by Yüzer et al. [8] on the residual behaviour of a cement mortar; normal concretes also may

show a similar trend to increase in compressive strength, but conflicting data are reported by different authors [12, 13, 22–24]. As well, the decrease in elastic modulus with increasing temperature could in some way be expected, although only based on the current information about the residual parameters of concretes [14, 15].

Masonry Specimens

Uniaxial compressive tests under displacement control, following UNI EN 1052–1 standard, and diagonal compressive tests following ASTM E 519–81 standard were carried out on the samples for the characterization of masonry in

Table 3 Experimental data of flexural and compressive tests on mortar samples

Flexural and compressive tests—MORTAR		
Sample	$f_{mf,\theta}$ (N/mm ²)	$f_{mc,\theta}$ (N/mm ²)
M-NF-1	5.60	12.38; 12.91
M-NF-2	5.97	14.96; 13.44
M-NF-3	4.58	10.61; 13.72
average NF	5.38	13.00
standard deviation NF	0.587	1.333
relative standard deviation NF	0.109	0.103
M-F3-1	3.87	15.03; 14.29
M-F3-2	4.66	18.65; 18.36
M-F3-3	3.91	17.75; 16.73
average F3	4.14	16.80
standard deviation F3	0.363	1.643
relative standard deviation F3	0.088	0.098
M-F6-1	2.03	9.53; 8.60
M-F6-2	2.16	9.29; 10.03
M-F6-3	2.09	9.12; 9.01
average F6	2.09	9.26
standard deviation F6	0.053	0.444
relative standard deviation F6	0.026	0.048

Table 4 Experimental data of elastic modulus testing on mortar samples

Elastic modulus—MORTAR	
Sample	E_m (N/mm ²)
M-NF-1E	11784
M-NF-2E	12190
M-NF-3E	9408
average NF	11127
standard deviation NF	1227
relative standard deviation NF	0.110
M-F3-1E	8257
M-F3-2E	11191
M-F3-3E	10541
average F3	9996
standard deviation F3	1258.2
relative standard deviation F3	0.126
M-F6-1E	11731
M-F6-2E	2822
M-F6-3E	1331
average F6	5295
standard deviation F6	4591.7
relative standard deviation F6	0.867

compression and shear. Five exposed and three unexposed samples were employed for each kind of test. All these tests were performed by means of a 6000 kN maximum load press by Metrocom Engineering, with data control system.

Before the compressive tests, the upper and lower faces of the samples were rectified by a cement covering to improve the load transfer from the machine to the sample; an uniform load distribution was ensured as well by interposing a 40 mm thick steel plate between the sample and the upper platen. The vertical displacement of the platen was controlled by means of a LVDT transducer, while four extensometers were placed on the two largest faces of each tested sample to record the vertical displacements; the loading velocity was taken as 0.05 mm/s, and

each test was terminated when half the peak load value was reached within the post-peak branch. For each test, the values of compressive strength $f_{c,\theta}$, initial elastic modulus E_θ , peak strain $\varepsilon_{c1,\theta}$ and ultimate strain $\varepsilon_{c2,\theta}$ are listed in Table 5. $\varepsilon_{c2,\theta}$ is the strain value at which, in the post-peak branch, half the value of peak stress is reached; since at this value the tests were conventionally considered as ended, it represents the ultimate value of strain. Figure 9 shows all the stress-strain diagrams, where the values of increasing strain are calculated from the average of the displacements recorded by the four extensometers; from these diagrams, the value of initial elastic modulus was calculated as the average of the stress/strain ratio at one and two third of the maximum stress.

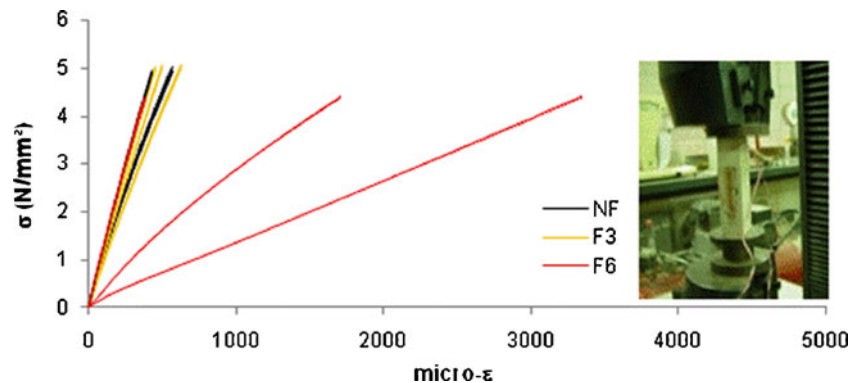
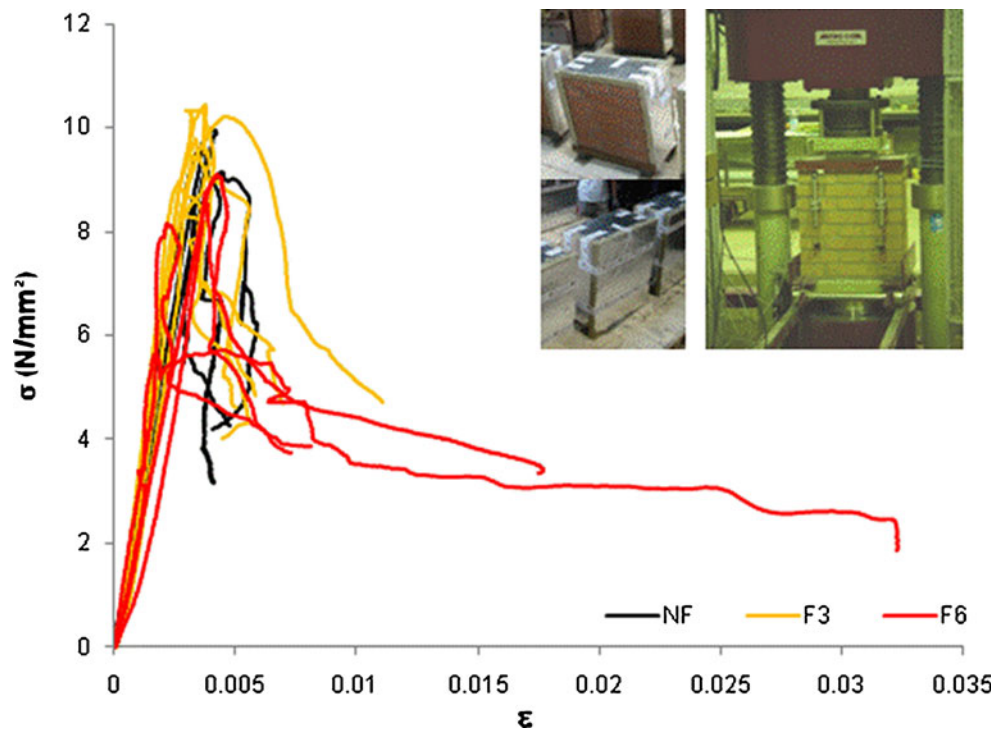
Fig. 8 Stress-strain diagram of elastic modulus tests on mortar samples

Table 5 Experimental data of compressive tests on masonry samples

Compressive tests—MASONRY				
Sample	$f_{c,\theta}$ (N/mm ²)	E_{θ} (N/mm ²)	$\varepsilon_{c1,\theta}$	$\varepsilon_{c2,\theta}$
2T-NF-1	9.64	2723	0.0037	0.0038
2T-NF-2	9.97	3085	0.0040	0.0039
2T-NF-3	9.13	2360	0.0044	0.0051
average NF	9.58	2723	0.0040	0.0043
standard deviation NF	0.346	295.98	0.00029	0.00059
relative standard deviation NF	0.036	0.109	0.072	0.138
2T-F3-1S-1	8.94	3293	0.0027	0.0056
2T-F3-1S-2	10.46	3246	0.0037	0.0054
2T-F3-1S-3	9.79	2874	0.0033	0.0069
2T-F3-1S-5	10.21	2438	0.0046	0.01
2T-F3-1S-6	10.31	3128	0.0030	0.0047
average F3	9.94	2996	0.0035	0.0065
standard deviation F3	0.548	314.45	0.00066	0.01358
relative standard deviation F3	0.055	0.105	0.189	2.089
2T-F6-1S-3	5.73	2687	0.0045	0.0265
2T-F6-1S-4	9.13	2246	0.0042	0.0085
2T-F6-1S-5	9.84	2736	0.0034	0.0083
2T-F6-1S-8	8.14	3131	0.0022	0.0064
2T-F6-1S-10	8.75	1771	0.0038	0.0058
average F6	8.32	2515	0.0036	0.0111
standard deviation F6	1.407	465.57	0.00080	0.00700
relative standard deviation F6	0.169	0.185	0.223	0.529

Concerning unexposed specimens, the increase in strain in the softening phase is generally small. Immediately

before the peak load, vertical cracks occurred in the bricks and at brick-mortar interfaces following the vertical

Fig. 9 Stress-strain diagram of compressive tests on masonry samples

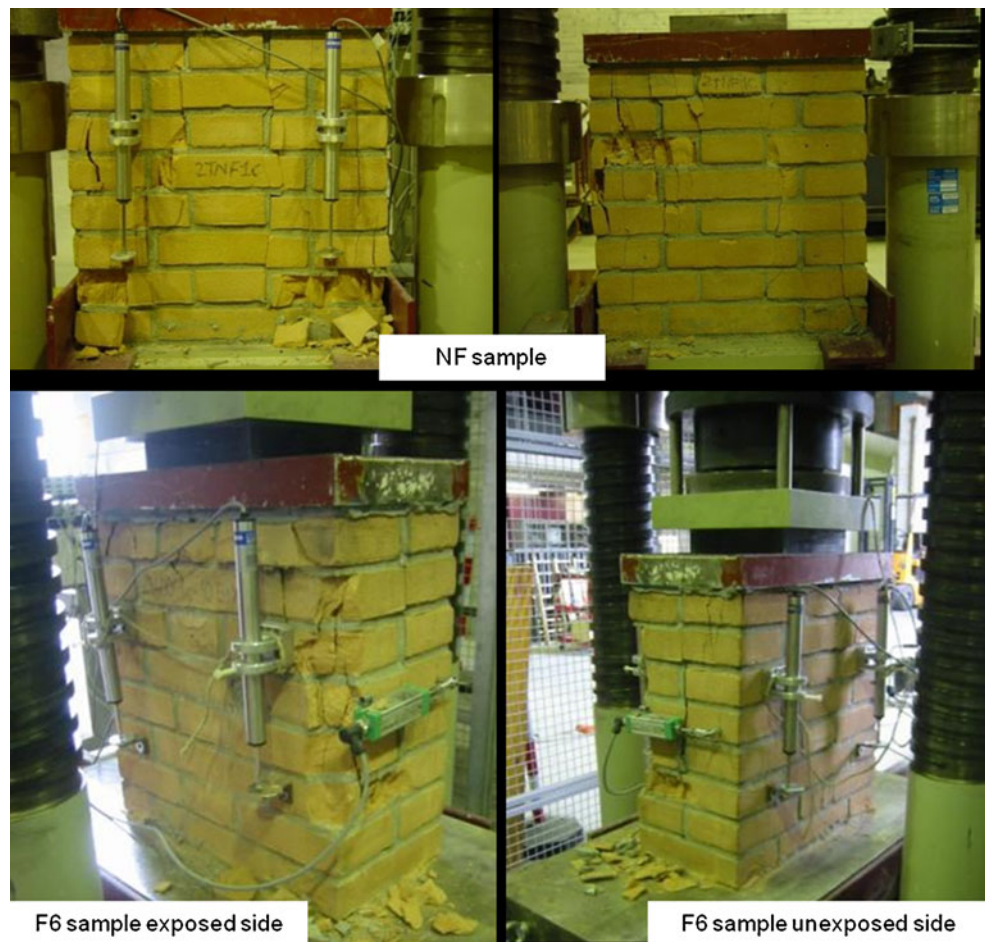
alignment of joints. During the performing of tests on F6 samples, cracks occurred first on the exposed side, immediately followed by superficial detachment of bricks; at the end of the tests, the damage of the exposed face was fairly greater. In a less evident way, this was also the behaviour of F3 samples. Moreover, at the peak stress, a vertical crack appeared along the middle of both lateral faces; after this was noticed, two additional extensometers were applied horizontally on the lateral faces of the remaining samples. The strength and stiffness of F3 masonry samples are slightly higher than NF (respectively +4% and +10%), while F6 samples show a decrease of -13% in strength and -7% in stiffness with respect to unexposed ones. The peak strain decreases (-12% in F3 and -10% in F6 cases), while the ultimate strain considerably increases with increasing temperature (+51 in F3 and +158% in F6 tests). Taking into consideration all the investigated properties except ultimate strain, their variations between NF and F3 specimens can be considered small; on the opposite side, the great increase in ultimate strain of both F3 and F6 samples points out that the softening phase is markedly influenced by exposure effects. The properties of F6 samples seem to indicate that at 600°C a not

negligible influence of thermal damage on the mechanical strength begins to appear. Figure 10 shows an exposed and an unexposed specimen after testing.

The pre-peak and peak behaviour was analysed in detail by evaluating the distribution of vertical strain at $0.33f_{c,\theta}$, $0.66f_{c,\theta}$ and $f_{c,\theta}$ following the recordings of each vertical extensometer; the distribution of horizontal strain, where it was measured, was evaluated too. A representation of this analysis is given in Figs. 11, 12 & 13, on the cross-section of each sample, where abbreviations are: v, h: vertical, horizontal extensometer; ex, un: exposed, unexposed side; sx, dx: left-, right-positioned. The positioning on the samples' faces is also schematically represented in each figure. The data of vertical strain at maximum stress $f_{c,\theta}$, which refer to the last rows of schemes in Figs. 11, 12 & 13, are also collected in Table 6. This analysis was carried out in order to clarify, with the help of recorded strain data, the concentration of mechanical damage at the exposed side which was evident in some cases.

Provided that the uniformity in the distribution of compressive load at the top of the sample had been assured, the uniformity of strain distribution, which is good in the unexposed samples (Fig. 11), is related to the temperature

Fig. 10 Both sides of unexposed (NF) and exposed (F6) specimens after the compressive test



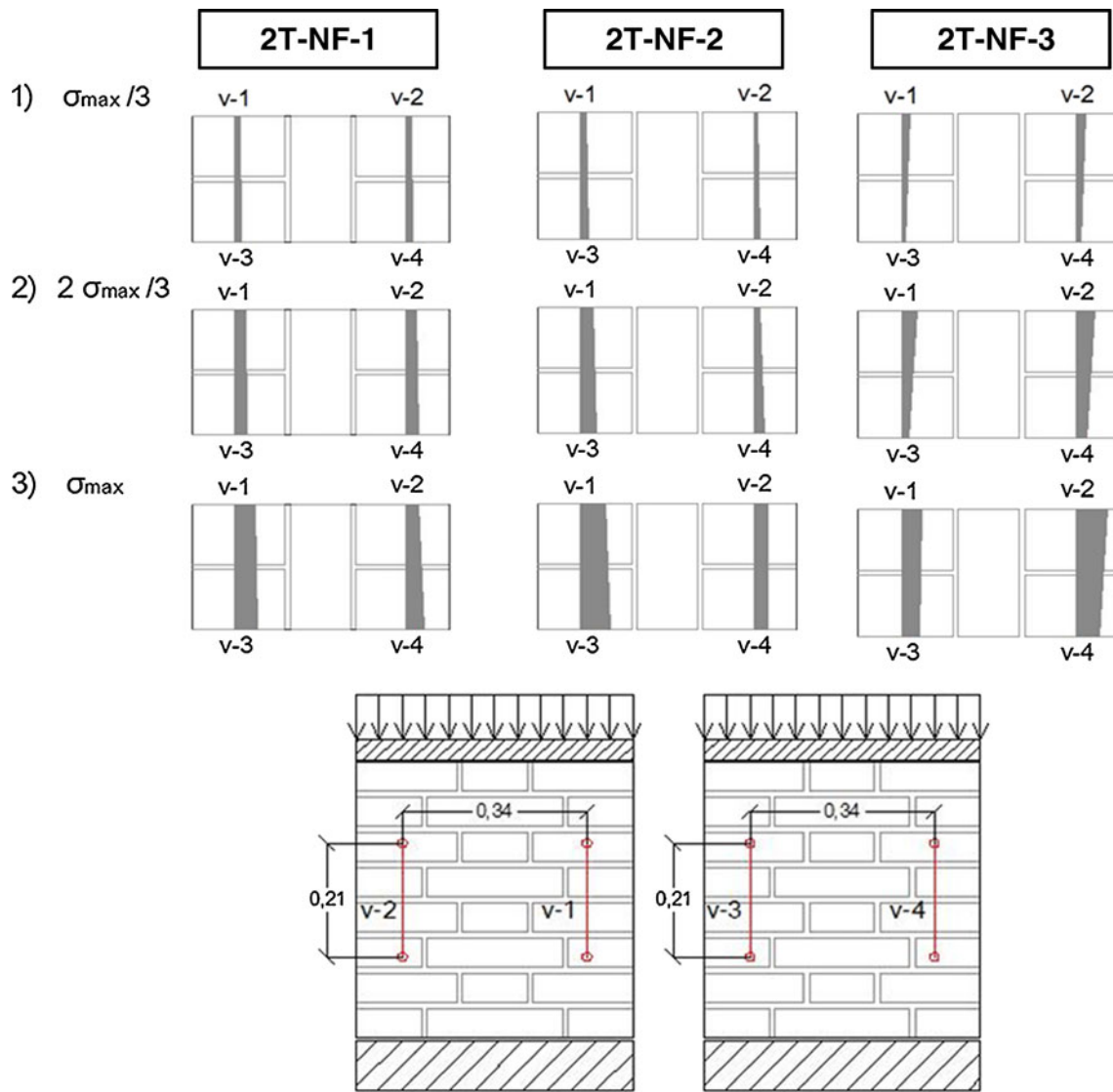


Fig. 11 Distribution of strain—NF specimens

of exposure. The results confirm that exposed specimens have generally larger vertical deformations at the exposed side. This asymmetrical distribution (Figs. 12–13) can be seen as a consequence of thermal damage that affected the exposed side. The samples with the most uneven strain distribution (e.g. 2T-F3-3, 2T-F6-8) have most notably shown the concentration of mechanical damage on the exposed side at failure; at the end of the test, the detachment of the thermally damaged thickness of the specimen was visible on the exposed side (see also Fig. 10 above). Looking at the last two columns of Table 6, reporting the mean values of strain on each of the two faces of the samples, the occurrence of greatest compressive deformation at the exposed side is frequent; in such cases, a decrease in elastic modulus in the thermally damaged thickness can be inferred, likely due to thermally induced cracking which mostly occurred at brick-joint interfaces

and, in 600°C exposed samples, also in bricks. The detachment of the thermally damaged thickness after exposure was already observed in ceramic materials by Gei et al. [25].

The presence of this high-temperature affected thickness can thus noticeably influence the strain behaviour of exposed masonry—the difference between the mean strain values of the two sides are greater for exposed masonry—even if the failure mode is the same as for unexposed (vertical cracks first occurring along the joint alignment, as above said).

The compressive failure is also accompanied by asymmetrical horizontal strain on the shortest sides, which accounts for cracking in the planes parallel to the exposed side.

Diagonal compressive tests on unexposed samples were performed at a velocity of 0.008 mm/s; the vertical and horizontal displacements were recorded by cross-placed extensometers along the diagonals of the two faces. The

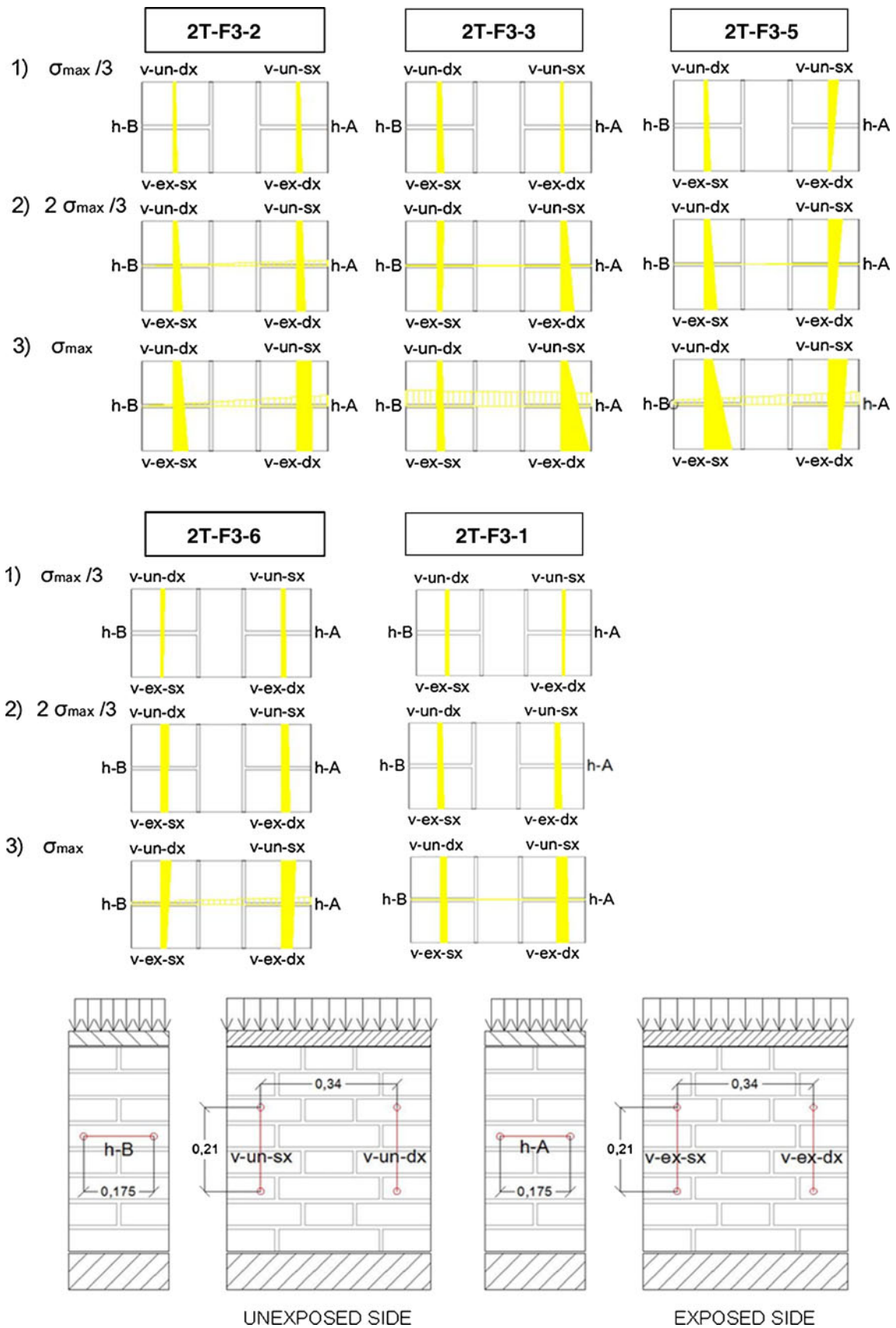


Fig. 12 Distribution of strain—F3 specimens

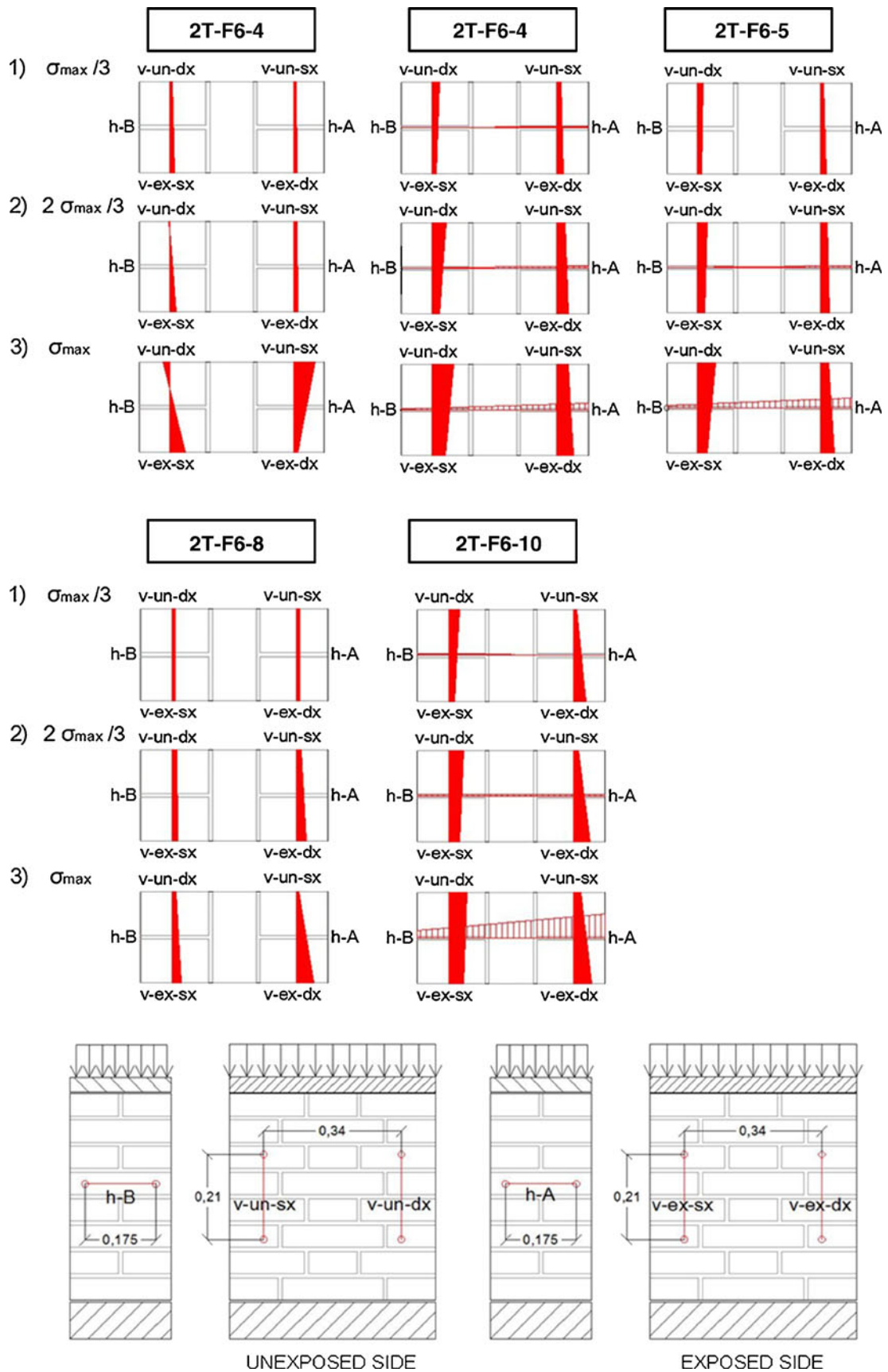


Fig. 13 Distribution of strain—F6 specimens



Table 6 Compressive strain distribution

Vertical strain distribution at collapse—MASONRY						
Sample	v1 unexposed side	v2 unexposed side	v3 unexposed side	v4 unexposed side	(v1+v2)/2	(v3+v4)/2
2T-NF-1	0.0041	0.0025	0.0046	0.0036	0.0033	0.0041
2T-NF-2	0.0049	0.0027	0.0057	0.0029	0.0038	0.0043
2T-NF-3	0.0039	0.0061	0.0034	0.0046	0.0050	0.0040
	unexposed side	unexposed side	exposed side	exposed side	(v1+v2)/2 unexposed	(v3+v4)/2 exposed
2T-F3-1S-1	0.0031	0.0020	0.0021	0.0036	0.0026	0.0029
2T-F3-1S-2	0.0040	0.0022	0.0042	0.0044	0.0031	0.0043
2T-F3-1S-3	0.0018	0.0014	0.0022	0.0080	0.0016	0.0051
2T-F3-1S-5	0.0052	0.0022	0.0075	0.0035	0.0037	0.0055
2T-F3-1S-6	0.0042	0.0029	0.0015	0.0033	0.0036	0.0024
2T-F6-1S-3	0.0060	-0.0018	0.0043	0.0013	0.0021	0.0028
2T-F6-1S-4	0.0031	0.0059	0.0035	0.0044	0.0045	0.0040
2T-F6-1S-5	0.0021	0.0050	0.0026	0.0037	0.0036	0.0032
2T-F6-1S-8	0.0006	0.0011	0.0026	0.0046	0.0009	0.0036
2T-F6-1S-10	0.0021	0.0050	0.0042	0.0049	0.0036	0.0046

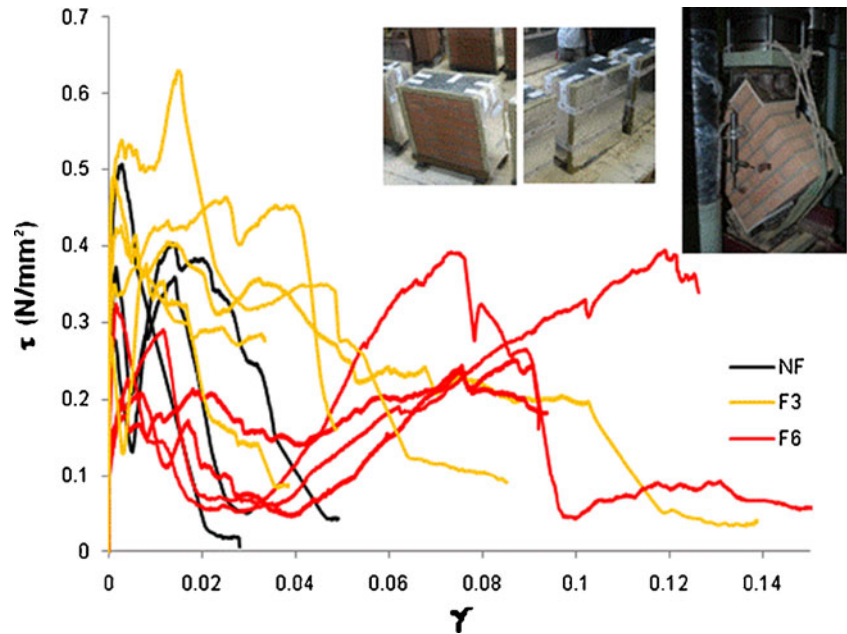
shear stress τ and shear strain γ were calculated from the recorded data following the reference standard ASTM E 519–81. The results of diagonal compressive tests, i.e. first

peak stress $\tau_{1,\theta}$, shear strength $f_{v0,\theta}$ (corresponding to the maximum stress value), shear modulus G_θ and peak strain $\gamma_{1,\theta}$ are listed in Table 7, while Fig. 14 shows the

Table 7 Experimental data of diagonal compressive tests on masonry samples

Diagonal compressive tests—MASONRY				
Sample	$\tau_{1,\theta}$ (N/mm ²)	$f_{v0,\theta}$ (N/mm ²)	G_θ (N/mm ²)	$\gamma_{1,\theta}$
2T-NF-4	0.51	0.51	3295	0.0029
2T-NF-5	0.37	0.39	2052	0.0016
2T-NF-6	0.28	0.40	2273	0.0140
average NF	0.39	0.43	2540	0.0062
standard deviation NF	0.0946	0.060	541.44	0.00556
relative standard deviation NF	0.243	0.140	0.2131	0.8975
2T-F3-1S-4	0.49	0.49	1235	0.001
2T-F3-1S-7	0.35	0.47	882	0.025
2T-F3-1S-8	0.42	0.43	852	0.0029
2T-F3-1S-9	0.28	0.38	606	0.0082
2T-F3-1S-10	0.54	0.63	833	0.015
average F3	0.42	0.48	882	0.0104
standard deviation F3	0.094	0.083	202.03	0.0088
relative standard deviation F3	0.225	0.175	0.22	0.84
2T-F6-1S-1	0.18	0.25	516	0.0867
2T-F6-1S-2	0.32	0.39	503	0.1193
2T-F6-1S-6	0.29	0.39	142	0.0735
2T-F6-1S-9	0.20	0.24	666	0.0744
average F6	0.25	0.32	457	0.0885
standard deviation F6	0.0590	0.073	192.68	0.0185
relative standard deviation F6	0.236	0.227	0.421	0.2096

Fig. 14 Shear stress-strain diagram of diagonal compressive tests on masonry samples



corresponding stress-strain diagrams. The shear modulus was calculated as the average of the stress-strain ratio at one and two third of the first maximum stress value.

Like it happened in compressive tests, the shear strength slightly increases in F3 (+12%) and decreases in F6 samples (−26%). The shear modulus suffers a significant decay with increasing temperature of exposition (F3: −65% and F6: −82%). Generally, concerning the shear stress-strain behaviour, both exposed and unexposed masonry samples underwent a stress drop after a first peak, and then slowly reached the maximum shear stress; at the first peak, cracks appeared both in bricks and at brick-vertical joint interfaces in unexposed samples, while interface cracking prevailed in the exposed samples, especially in F6 cases. Moreover, this occurred at remarkably lower shear stress values for exposed samples. Then, the subsequent slow load increase was accompanied by slipping along the bed joints, until the maximum shear stress was reached and the specimen showed wide gaps between bricks and vertical joints as well as indentation due to sliding along the middle horizontal joint. The tests were interrupted on the subsequent descending branch; in the case of diagonal compression, a common test

end criterion could not be observed for instruments' safety reasons. Figure 15 shows a comparison between an exposed and an unexposed sample after testing.

The concentration of cracking at interfaces, together with lower first peak stress values, indicates a loss of brick-mortar cohesion in the exposed samples; this phenomenon can be linked to the interface cracking, as an effect of fire exposure, observed in the samples' exposed surfaces just after the thermal cycle.

In this case again, the fairest difference resorting from the diagrams lies in the longer post peak branches of exposed masonry samples. Moreover, F3 and F6 samples reached the maximum stress at much larger strain values than unexposed ones. The repeated increase-decrease in stress, which originate a saw-shaped diagram, is a well-known phenomenon in diagonal compressive tests. It can be ascribed to the combined strength contributions of brick-mortar cohesion (decreasing with the growth of interface cracks) and friction along the bed joints. This could be seen in all the tested samples NF, F3 and F6, but the phenomenon appears quite magnified with increasing temperature of exposure; in fact, in F6 samples (red lines in Fig. 14) noticeable increases in stress begin at

Fig. 15 Exposed and unexposed specimens after diagonal compressive tests

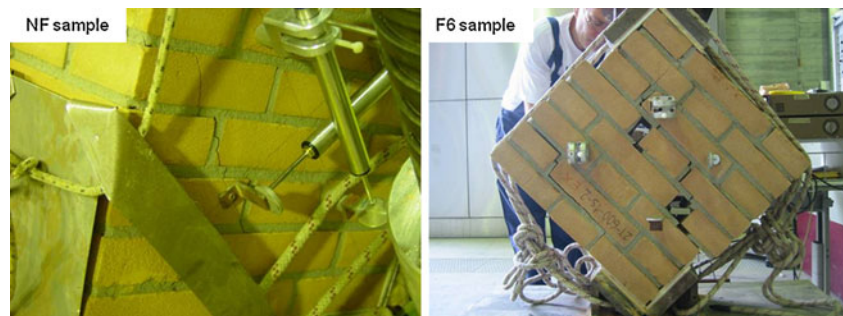


Table 8 Ratios of original/residual material properties

Factors of original property		F3	F6
BRICK	$f_{bc,\theta} / f_{bc}$	0.91	0.62
	$E_{b,\theta} / E_b$	1.15	1.01
MORTAR	$f_{mf,\theta} / f_{mf}$	0.77	0.39
	$f_{mc,\theta} / f_{mc}$	1.29	0.71
MASONRY	$E_{m,\theta} / E_m$	0.90	0.48
	$f_{c,\theta} / f_c$	1.04	0.87
	E_θ / E	1.10	0.93
	$\varepsilon_{c1,\theta} / \varepsilon_{c1}$	0.88	0.90
	$\varepsilon_{c2,\theta} / \varepsilon_{c2}$	1.51	2.58
	$f_{v0,\theta} / f_{v0}$	1.12	0.74
	G_θ / G	0.35	0.18
	$\gamma_{1,\theta} / \gamma_1$	1.68	14.27

strain values around 0.03. In those cases, since the first dropping occurs at lower values of stress than NF and F3 samples, evidence can be found that the high temperature exposure has most affected the brick-mortar cohesion, while friction still appears to give an appreciable contribution to the strength of the sample. The high values of strain generally reached by the exposed samples at the highest stress values can be interpreted as a reinforcement of the shear softening instability of the specimen due to the effect of thermal damage.

Finally, the displacement data revealed no appreciable difference between exposed and unexposed faces. Table 8 presents the ratios between original and residual values of all the mechanical properties.

Experimental Functions of Mechanical Decay

The factor of original property k_θ indicates the ratios (previously listed in Table 8) between each residual mechanical parameter and the original one, for brick, mortar and masonry. For each property, a function of mechanical decay with increasing temperature of exposure (k_θ - θ functions) was defined based on the above reported data on 300°C and 600°C exposure. These functions express a possible evolution of the respective k_θ ratio on the basis of the known values; parabolic and exponential functions were chosen according to the identified trend of each parameter, as follows (subscripts ₃₀₀ and ₆₀₀ denote residual values at 300°C and at 600°C):

1. $k_{300} > 1$, $k_{600} > k_{300}$ ($f_{c,\theta}$, E_θ , $f_{v,\theta}$, $f_{mc,\theta}$, $E_{b,\theta}$)
2. $k_{300} < 1$, $k_{600} > 1$ (ε_{c1})
3. $k_{300} < 1$, $k_{600} < 1$ (G_θ , $f_{bc,\theta}$, $f_{mf,\theta}$, $E_{m,\theta}$)

4. $k_{300} > 1$, $k_{600} > 1$ ($\varepsilon_{c2,\theta}$, $\gamma_{1,\theta}$)

Thus the following k_θ - θ relations express the temperature-dependent decay for each mechanical parameter:

- compressive strength of masonry ($f_{c,\theta}$)

$$k_\theta = \frac{f_{c,\theta}}{f_c} = -(1.0 \cdot 10^{-6})\theta^2 + (5.0 \cdot 10^{-4})\theta + 0.9898 \quad (1)$$

- initial elastic modulus of masonry (E_θ)

$$k_\theta = \frac{E_\theta}{E} = -(2.0 \cdot 10^{-6})\theta^2 + (9.0 \cdot 10^{-4})\theta + 0.9833 \quad (2)$$

- peak compressive strain of masonry ($\varepsilon_{c1,\theta}$)

$$k_\theta = \frac{\varepsilon_{c1,\theta}}{\varepsilon_{c1}} = (9.0 \cdot 10^{-7})\theta^2 + (7.0 \cdot 10^{-4})\theta + 1.0144 \quad (3)$$

- ultimate compressive strain of masonry ($\varepsilon_{c2,\theta}$)

$$k_\theta = \frac{\varepsilon_{c2,\theta}}{\varepsilon_{c2}} = (3.0 \cdot 10^{-6})\theta^2 + (9.0 \cdot 10^{-4})\theta + 0.9816 \quad (4)$$

- shear strength of masonry ($f_{v0,\theta}$)

$$k_\theta = \frac{f_{v0,\theta}}{f_{v0}} = -(0.3 \cdot 10^{-5})\theta^2 + (1.4 \cdot 10^{-3})\theta + 0.9739 \quad (5)$$

- tensile strength of masonry ($f_{t,\theta}$)

$$k_\theta = \frac{f_{t,\theta}}{f_t} = -(0.3 \cdot 10^{-5})\theta^2 + (1.3 \cdot 10^{-3})\theta + 0.9762 \quad (6)$$

- shear modulus of masonry (G_θ)

$$k_\theta = \frac{G_\theta}{G} = 0.9826 \cdot e^{-0.003 \cdot \theta} \quad (7)$$

- peak shear strain ($\gamma_{1,\theta}$)

$$k_\theta = \frac{\gamma_{1,\theta}}{\gamma_1} = 0.7006 \cdot e^{0.0046 \cdot \theta} \quad (8)$$

- compressive strength of brick ($f_{bc,\theta}$)

$$k_\theta = \frac{f_{bc,\theta}}{f_{bc}} = -(1.0 \cdot 10^{-6})\theta^2 + (3.0 \cdot 10^{-5})\theta + 0.9998 \quad (9)$$

- initial elastic modulus of brick ($E_{b,\theta}$)

$$k_\theta = \frac{E_{b,\theta}}{E_b} = -(2.0 \cdot 10^{-6})\theta^2 + (1.1 \cdot 10^{-3})\theta + 0.9789 \quad (10)$$

- compressive strength of mortar ($f_{mc,\theta}$)

$$k_\theta = \frac{f_{mc,\theta}}{f_{mc}} = -(5.0 \cdot 10^{-6})\theta^2 + (2.7 \cdot 10^{-3})\theta + 0.9486 \quad (11)$$

- flexural strength of mortar ($f_{mf,\theta}$)

$$k_\theta = \frac{f_{mf,\theta}}{f_{mf}} = -(8.0 \cdot 10^{-7})\theta^2 + (6.0 \cdot 10^{-4})\theta + 1.0118 \quad (12)$$

- initial elastic modulus of mortar ($E_{m,\theta}$)

$$k_\theta = \frac{E_{m,\theta}}{E_m} = -(2.0 \cdot 10^{-6})\theta^2 + (2.0 \cdot 10^{-4})\theta + 0.9964 \quad (13)$$



These functions are graphically represented in the diagrams of Figs. 16–17, in the range 20–600°C.

As it can be seen from the graphs, $f_{c,\theta}$ and $f_{v0,\theta}$ increase at 300°C and decrease at 600°C similarly to the strength of the mortar $f_{mc,\theta}$, while the elastic modulus $E_{c,\theta}$ follows the same trend as $E_{b,\theta}$. In both cases, the variations in the properties of masonry are smaller than those of components. As well, the tensile and shear strength of masonry show a trend similar to the compressive strength of mortar; the shear modulus progressively decays similarly to the elastic modulus of mortar. The great increase in peak strain both in compression and in shear ($\varepsilon_{c1,\theta}$, $\varepsilon_{c2,\theta}$, $\gamma_{1,\theta}$) is of such entity that can't totally be ascribed to the variations in stiffness and strength of the two components; more likely, a different mechanical stress redistribution in the exposed masonry assemblies could have been induced by thermal micro-cracking. As above said, local losses of brick-mortar cohesion were actually detected in the masonry samples just after thermal cycles as the prevailing phenomenon of thermal damage. Moreover, this may also be the reason of the great decrease in shear modulus with increasing temperature; diagonal compressive tests showed that, since the early stage of collapse, interface detachment becomes more frequent than brick cracking as the temperature of exposition increases.

The observed collapse behaviour of exposed masonry samples under uniaxial compression—with the asymmetrical distribution of vertical strain at the peak—put into evidence that the thickness of weakened material at the exposed side is markedly increased after 600°C exposure.

The mechanical decay is quantified by the k_θ factor, meaning the ratio between residual and original property. The values of k_θ at 300°C and 600°C for each property provided the basis for the formulation of the respective equations of mechanical decay in function of the external temperature θ . These functions are a first attempt to define the development of temperature-dependent decay, since

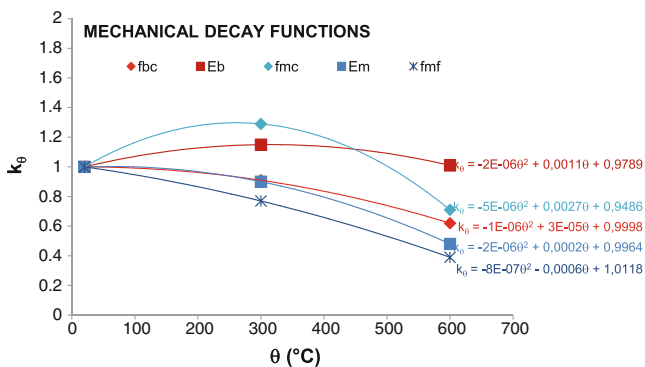


Fig. 16 $k_\theta - \theta$ diagrams for the mechanical properties of brick and mortar

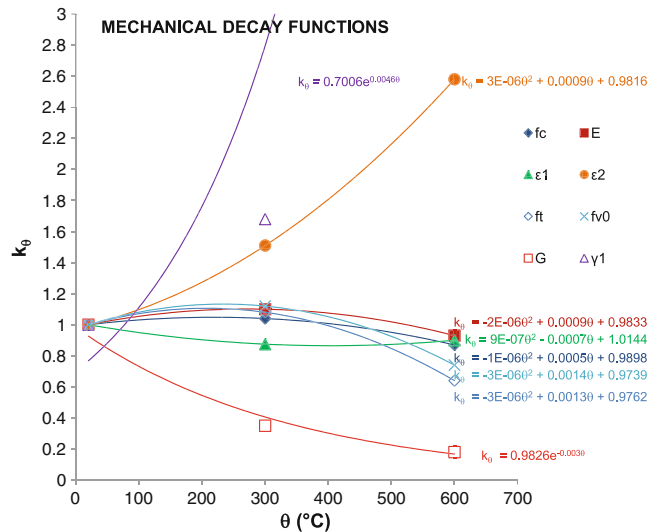


Fig. 17 $k_\theta - \theta$ diagrams for the mechanical properties of masonry

they are based on the experimental values at 20, 300 and 600°C; their reliability may be improved by further experimental research taking into account intermediate and higher temperatures.

Conclusions

Currently, there is a lack of experimental information about the residual mechanical performances of masonry and clay bricks after high temperature exposition. The experimental programme here described, which is the first part of a wider research, provides new experimental data on the residual mechanical properties of one type of masonry, made of traditional bricks and cement mortar and having a thickness of 25 cm, considered as a load-bearing wall having the function of fire compartment, i.e. exposed to high temperature on one side. Two maximum temperature conditions, i. e. 300 and 600°C, have been accounted for, in order to represent low-medium levels of exposition; to the purpose of setting up the functions of properties' decay with increasing temperature ($k_\theta - \theta$ functions), it was preferable not to investigate severe situations, in order to enlighten the initial evolution of residual parameters in function of temperature. The heating rate (19°C/min) and duration at maximum temperature (1 h) were chosen in order to simulate 'short-fire' conditions as features of an accidental exposure. The thermal cycles adequately reproduced, as it could be seen from temperature recordings, the situation of a load-bearing separating masonry wall.

After the performing of thermal cycles, the masonry samples showed clear signs of thermal damage on the exposed side, i.e. interface cracking and, in 600°C-exposed samples, micro-cracks in bricks and mortar joints. During the subsequent mechanical tests, the



mechanical behaviour up to failure could be observed in the different cases:

- *Uniaxial compressive tests:* In all unexposed and exposed cases, vertical cracks along the alignment of central mortar joints appeared at incipient failure; this feature of behaviour should be ascribed to the peculiar masonry pattern. Subsequently, superficial detachments of bricks at the exposed surfaces of F3 and particularly F6 samples were observed, due to the entity of the superficial thickness damaged by high temperature exposure. The decay in compressive strength can be considered of relevance in 600°C-exposed samples. The stress-strain diagrams showed longer descending branches in both cases of exposed masonry, leading to high values of ultimate strain.
- *Diagonal compressive tests:* As the first signs of failure, exposed samples showed a clear prevalence of brick-joint interface cracking; vertical cracks in bricks were almost absent in F6 samples. The decay of mechanical strength after exposure to 600°C is considerable; the shear stiffness was found to decrease dramatically even after 300°C-exposure. A huge increase in strain at maximum stress values could be observed in all the exposed samples.

The following Tables 9, 10, & 11 recollect the per cent differences in the mean values of all the investigated properties of exposed materials with respect to the unexposed. Concerning bricks, the increase in stiffness after 300°C-exposure (which is almost completely lost after 600°C-exposure) can be related to the parallel decrease in compressive strength; the bricks' strain capacity in the elastic field is thus certainly reduced by exposure to low-medium levels of high temperature. The experimental results of mortar samples have shown to agree with data from other similar researches; a progressive decay was found to affect the flexural strength and the compressive stiffness with increasing temperature of exposure. After 600°C-exposure, the decrease in all the properties is clearly appreciable. The tendency of compressive strength—being higher than the original in F3 and lower in F6 samples—was found not to be uniform at low-medium levels of high temperature, as it was already demonstrated by other researches on cement materials. The differences in compressive strength and stiffness of masonry remain relatively small if compared to those of components. The general

Table 9 Per cent differences in residual mechanical properties—BRICKS

BRICKS		
Property	% F3	%F6
compressive strength	−9	−38
elastic modulus	+15	+1

Table 10 Per cent differences in residual mechanical properties—mortar

MORTAR		
Property	% F3	%F6
flexural strength	−23	−61
compressive strength	+29	−29
elastic modulus	−10	−51

mechanical decay after 600°C-exposure was clearly ascertained. The remarkable increase in ultimate compressive strain and peak shear strain ($\varepsilon_{c,2,\theta}$ and $\gamma_{l,\theta}$ parameters) at growing temperatures can be related to the observed features of thermally induced damage on the exposed surfaces of masonry samples. The pre-existing cracking and micro-cracking can well originate a loss of stiffness affecting the whole stress-strain behaviour in diagonal compression and the post-elastic field in compression (where the brick-mortar cohesion gives a less important contribution to strength); this can lead to the abnormal augmentation of $\varepsilon_{c,2,\theta}$ and $\gamma_{l,\theta}$ and thus to a fictitious increase in strain capacity.

The immediately following steps of the present research are aimed to elaborate a theoretical-experimental constitutive law expressing the residual behaviour of this physical model of masonry in compression (load-bearing fire-separating wall 25 cm thick) on the basis of the experimental decay laws. The first formulation of this constitutive law will be presented in a further study; it will be the first step to build a general model for the residual behaviour of masonry in function of the temperature of exposure; it will be progressively refined by the experimental testing and analysis of other cases (i.e. load-bearing fire-separating wall 38 cm thick, load-bearing non-separating wall 25 cm thick and load-bearing non-separating wall 38 cm thick) which will be dealt with in the whole research. It can be expected that the k_θ coefficient of residual strength (both in

Table 11 Per cent differences in residual mechanical properties—MASONRY

MASONRY		
Property	% F3	%F6
compressive strength	+4	−13
elastic modulus	+10	−7
peak strain	−12	−10
ultimate strain	+51	+158
tensile strength	+8	−36
shear strength	+12	−26
shear elastic modulus	−65	−82
peak shear strain	+68	+1327

compression and in shear) will noticeably increase with increasing wall thickness, within the same exposure condition; then, the stress-strain diagrams can show different shapes depending on the masonry pattern and the entity of damage.

The general model of the residual behaviour of masonry, composed by the mechanical decay functions and the temperature-dependent compressive law, is intended to provide a basis for the design and verification of buildings whose safety had to be assured after a fire event, and for the evaluation of the residual level of reliability of masonry structures subjected to fire. The proposed laws of mechanical decay can potentially apply to the study of new as well as historic masonry, since the choice of components and pattern can well fit to comparisons to both existing buildings and modern materials. Indeed, as above said, a refinement of the functions can be attained by tests on brick, mortar and masonry after exposure at other values of maximum temperature; the initial evolution of the residual mechanical parameters (especially the compressive and shear strength of masonry and compressive strength of mortar) could thus be clarified in a better way, as well as the entity of decay beyond 600°C. Moreover, a parametric study on the exposure conditions could add information on the residual behaviour of masonry after high temperature exposure; reasonably, increases in duration at maximum temperature will result in decreases in mechanical properties, but the effects of a longer duration can be expected to be less important than those of a higher maximum temperature; investigations on different cooling regimes could be very useful to understand the effects of the extinguishment of a fire, since the thermal shock due to rapid water cooling can likely worsen the mechanical decay with respect to slow air cooling.

Finally, from the experimental observations here presented, the role played by the pre-existing thermal damage within the mechanical behaviour of masonry can be inferred. The quantification of the damaged thickness can thus be a key topic for the development of the research here dealt with. The thickness weakened by the exposure should be related to maximum temperature and, additionally, duration and cooling regime, within cross-section experimental analyses of masonry samples. It can be expected that once a dependency of the weakened thickness from temperature is identified, the temperature-dependent model of masonry could be formulated in an even more general way, i.e. in function of the ratio between weakened and global thickness of the wall.

Acknowledgements The authors would like to thank Terreal Italia—San Marco Laterizi s.r.l., Noale (VE), for the support, and all the technicians at the Laboratory of Strength of Materials (LabSCo) of IUAV University of Venice.

References

- Rossi V (2003) La sicurezza del patrimonio culturale in caso di incendio. Built heritage and its protection—43th International Fire-fighters' Workshop, Moreton in Marsh, UK, 30th September–2nd October 2003
- Bukowski RW, Nuzzolese V, Bindo M (2003) Performance-based fire protection of historical structures, Proc. Forum for International Cooperation on Fire Research, October 23rd, 2001, Milan, Italy, pp39–51
- Nassi L (2006) Sistemi antincendio nelle biblioteche e negli edifici storici, Proc. Convegno nazionale AntIncendio, Roma (in Italian)
- CSE-ANDIL (1995) Ricerca sperimentale per la determinazione della resistenza al fuoco di varie tipologie di solai e pannelli murari con elementi di laterizio, svolta in collaborazione con ANDIL—AssoLaterizi, Centro Studi ed Esperienze Antincendi—Roma (in Italian)
- Russo S, Boscato G, Sciarretta F (2008) Behaviour of a historical masonry structure subjected to fire. *Mason Int* 21(1):1–14
- Sciarretta F (2010) Analisi teorico-sperimentale di muratura malta-mattoni soggetta ad alte temperature. PhD dissertation, University of Trento (in Italian)
- Abrams MS (1979) Behavior of inorganic materials in fire. In: Smith EE, Harmathy TZ (eds) Design of buildings for fire safety. A symposium sponsored by ASTM committee E05 for fire standards. ASTM STP 685, pp14–73
- Yüzer N, Aköz F, Öztürk LD (2004) Compressive strength—color change relation in mortars at high temperature. *Cem Concr Res* 34:1803–1807. doi:10.1016/j.cemconres.2004.01.015
- Felicetti R, Gambarova PG (1998) Effects of high temperature on the residual compressive strength of high-strength siliceous concretes. *ACI Mater J* 95-M37:395–406
- Bingöl AF, Gül R (2008) Effect of elevated temperatures and cooling regimes on normal strength concrete. *Fire Mater* 33:79–88. doi:10.1002/fam.987
- Cülfik MS, Özturan T (2002) Effect of elevated temperatures on the residual mechanical properties of high-performance mortar. *Cem Concr Res* 32:809–816
- Arioz O (2007) Effect of elevated temperatures on properties of concrete. *Fire Saf J* 42:516–522. doi:10.1016/j.fire saf.2007.01.003
- Felicetti R, Colombo M (2006) Nuove tecniche non distruttive per la stima del danno da incendio nelle strutture in calcestruzzo armato. In: Russo S, Siviero E (eds) Convegno nazionale Sperimentazione su Materiali e Strutture, Università IUAV di Venezia, pp 53–63 (in Italian)
- Xiao J-Zh, König G (2004) Study on concrete at high temperatures in China—an overview. *Fire Saf J* 39:89–103. doi:10.1016/S0379-7112(03)0093-6
- Baker G (1996) The effect of exposure to elevated temperatures on the fracture energy of plain concrete. *Mater Struct* 29:383–388
- RILEM Technical Committee (2007) Recommendation of RILEM TC 200 HTC: mechanical concrete properties at high temperatures—modelling and applications Part 2: stress-strain relation. *Mater Struct* 40:855–864. doi:10.1617/s11527-007-9286-1
- Drysdale D (1999) An introduction to fire dynamics, 2nd edn. Wiley & sons, Chichester
- Nadjai A, O'Garra M, Ali FA, Jurgen R (2006) Compartment masonry walls in fire situations. *Fire Technol* 42:211–231. doi:10.1007/s10694-006-7509-6
- Nguyen ThD, Meftah F, Chammas R, Mebarki A (2009) The behaviour of masonry walls subjected to fire: modelling and

- parametric studies in the case of hollow burnt-clay bricks. *Fire Saf J* 44:629–641. doi:[10.1016/j.firesaf.2008.12.006](https://doi.org/10.1016/j.firesaf.2008.12.006)
20. Russo S, Sciarretta F (2009) Residual strength of traditional brick masonry subjected to high temperatures. In: Mazzolani F (ed) *Protection of historical buildings—ProHiTech 09*, Rome, 2009, Balkema, pp 1417–1422
 21. CEN/TC 250 (2005) *Eurocode 6: design of masonry structures—Part 1–2: general rules—structural fire design*, UNI EN 1996-1-2
 22. Phan LT, Carino NJ (2003) Code provisions for high strength concrete strength-temperature relationship at elevated temperatures. *Mater Struct* 36:91–98
 23. Husem M (2006) The effects of high temperature on compressive and flexural strength of ordinary and high performance concrete. *Fire Saf J* 41:155–163. doi:[10.1016/j.firesaf.2005.12.002](https://doi.org/10.1016/j.firesaf.2005.12.002)
 24. Yang H, Lin Y, Hsiao Ch, Liu J-Y (2009) Evaluating residual compressive strength of concrete at elevated temperatures using ultrasonic pulse velocity. *Fire Saf J* 44:121–130. doi:[10.1016/j.firesaf.2008.05.003](https://doi.org/10.1016/j.firesaf.2008.05.003)
 25. Gei M, Bigoni D, Guicciardi S (2004) Failure of silicon nitride under uniaxial compression at high temperature. *Mech Mater* 36:335–345. doi:[10.1016/S0167-6636\(03\)00063-2](https://doi.org/10.1016/S0167-6636(03)00063-2)